PHYSICAL REVIEW VOLUME 74, NUMBER 9 NOVEMBER 1, 1948

Line Shapes in Nuclear Paramagnetism

G. E. PAKE*† AND E. M. PURCELL
Lyman Laboratory of Physics, Harvard University, Cambridge, Massachusetts

(Received July 6, 1948)

This note discusses briefly several methods of describing the width and shape of the resonances characteristic of nuclear paramagnetism. Use of the so-called moments of the shape function is illustrated by an experimental determination of a root mean square line width which is in substantial agreement with a calculation by Van Vleck. The solutions of the Bloch equations, which lead to the Lorentz shape function traditional in the theory of radiation- and collision-broadened lines, are compared with susceptibility curves based on a Gauss absorption curve. A significant difference between the two dispersion curves serves as a criterion for determining whether or not either of these two shapes closely approximates to a given experimental curve, and experimental examples of each are given.

For comparison of shape functions, several well-known specializations of the Kronig-Kramers relations are employed. The collection of these formulae may incidentally prove convenient and useful to those engaged in studies of nuclear paramagnetism.

INTRODUCTION

WHEN a sample containing nuclear magnetic moments is immersed in a constant magnetic field $\mathbf{H}_0$, energy may be absorbed from a radiofrequency magnetic field which is perpendicular to $\mathbf{H}_0$ and has a frequency near the nuclear Larmor frequency. The rate of absorption is proportional to the imaginary component of the nuclear magnetic susceptibility $\chi=\chi'-i\chi''$. The dependence of χ'' on frequency ν is given by the shape function $g(\nu)$, defined as follows:[1]

$$\left.\begin{aligned}\chi''(\nu)&=\pi\chi_0\nu_0 g(\nu)\\ \int_0^\infty g(\nu)d\nu&=1\\ T_2&=\tfrac{1}{2}[g(\nu)]_{\mathrm{Max}}.\end{aligned}\right\}. \quad (1)$$

Here $\chi_0=N\mu^2(3kT)^{-1}(I+1)/I$ is the static nuclear susceptibility and $\nu_0=(\mu H_0)/(Ih)$ is the resonant frequency for a nucleus with spin I and magnetic moment $\mu=g\beta I$, g being the nuclear g-factor and β the nuclear magneton. For a given shape function, the line width is proportional to $1/T_2$. If $\chi''(\nu)$ is known, $\chi'(\nu)$ is given by the first of the Kronig-Kramers relations:

$$\left.\begin{aligned}\chi'(\nu)-\chi'(\infty)&=\frac{2}{\pi}\int_0^\infty\frac{\nu'\chi''(\nu')d\nu'}{\nu'^2-\nu^2}\\ \chi''(\nu)&=-\frac{2\nu}{\pi}\int_0^\infty\frac{\chi'(\nu')-\chi'(\infty)}{\nu'^2-\nu^2}d\nu'.\end{aligned}\right\}. \quad (2)$$

These formulae were originally derived for the electric susceptibility.[2] Gorter and Kronig[3] later pointed out their validity for magnetism, and they are easily shown to apply to a large class of complex quantities used in the analysis of physics and engineering problems.[4]

In Eq. (2), as well as in Eqs. (3), (4), and (5) which follow, the Cauchy principal value is to be understood, that is, if $f(\nu')$ has a singularity at $\nu'=\nu$, then

$$\int_0^\infty f(\nu')d\nu'=\lim_{\delta\to 0}\left[\int_0^{\nu-\delta}f(\nu')d\nu'+\int_{\nu+\delta}^\infty f(\nu')d\nu'\right].$$

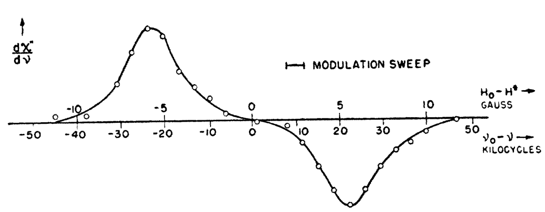

FIG. 1. Fluorine (F^{19}) resonance in a CaF_2 single crystal. $\mathbf{H}_0$ along [100]; $H^*=6824.2$ gauss, $\nu=27.33$ Mc.

* Predoctoral Fellow of the National Research Council.
† Now at Washington University, St. Louis, Missouri.
[1] N. Bloembergen, E. M. Purcell, and R. V. Pound, Phys. Rev. 73, 679 (1948).

[2] R. de L. Kronig, J. Opt. Soc. Am. 12, 547 (1926); H. A. Kramers, Atti del Congresso Internationale dei Fisici, Como, Vol. 2, 545 (1927). Compare also Radiation Laboratory Report 735 by J. H. Van Vleck, or Vol. 13, Radiation Laboratory Series (McGraw-Hill), Chap. 8.
[3] C. J. Gorter and R. de L. Kronig, Physica 3, 1009 (1936).
[4] H. W. Bode, *Network Analysis and Feedback Amplifier Design* (D. Van Nostrand and Company, New York, 1945), Chap. XIV.

SPECIAL FORMS OF THE KRONIG-KRAMERS RELATIONS

Both $\chi'(\nu)$ and $\chi''(\nu)$ for nuclear resonances are effectively zero except in a small frequency interval, usually no more than 200 kilocycles even for solids, about the resonant frequency ν_0 of at least several megacycles. The approximations $\nu'/(\nu'+\nu)\cong\frac{1}{2}$ and $\nu/(\nu'+\nu)\cong\frac{1}{2}$ therefore allow

$$\left.\begin{aligned}\chi'(\nu)&=\frac{1}{\pi}\int_0^\infty\frac{\chi''(\nu')d\nu'}{\nu'-\nu},\\ \chi''(\nu)&=-\frac{1}{\pi}\int_0^\infty\frac{\chi'(\nu')d\nu'}{\nu'-\nu}.\end{aligned}\right\}. \tag{3}$$

Placing $\nu'=\nu_0+\Delta\nu'$ and $\nu=\nu_0+\Delta\nu$ yields

$$\left.\begin{aligned}\chi'(\nu_0+\Delta\nu)&=\frac{1}{\pi}\int_{-\infty}^\infty\frac{\chi''(\Delta\nu')d(\Delta\nu')}{\Delta\nu'-\Delta\nu},\\ \chi''(\nu_0+\Delta\nu)&=-\frac{1}{\pi}\int_{-\infty}^\infty\frac{\chi'(\Delta\nu')d(\Delta\nu')}{\Delta\nu'-\Delta\nu}.\end{aligned}\right\}. \tag{4}$$

Extension of the lower limit from $-\nu_0$ to $-\infty$ adds negligibly to the integrals in view of the narrowness of the resonance. Formulae (4) are more conveniently applied to nuclear susceptibilities than the more general relations (2). Placing $(\nu'/\nu)-1\cong(\nu'-\nu)/\nu_0$ and using $\chi'(0)\ll\chi'(\nu_0)$ after partial integration of Eq. (3) yields

$$\left.\begin{aligned}\chi'(\nu)&=\frac{1}{\pi}\int_0^\infty\frac{d\chi''(\nu')}{d\nu'}\log\left|\frac{\nu_0}{\nu'-\nu}\right|d\nu',\\ \chi''(\nu)&=-\frac{1}{\pi}\int_0^\infty\frac{d\chi'(\nu')}{d\nu'}\log\left|\frac{\nu_0}{\nu'-\nu}\right|d\nu'.\end{aligned}\right\}. \tag{5}$$

The modulation type of apparatus developed by Purcell, Pound, and their co-workers[1,5] may be adjusted to measure quantities directly proportional to either of the derivatives involved in Eq. (5). If the available apparatus measures directly the derivative of but one part of the nuclear susceptibility, the relations (5) offer the most direct means of obtaining the other part. The form of the integrals in Eqs. (5), each of which has a logarithmic singularity in its integrand, also makes evident the qualitative similarity between one part of the susceptibility and the derivative of the other part.

[5] R. V. Pound, E. M. Purcell, and H. C. Torrey, Phys. Rev. **69**, 681 (1946).

TABLE I. Root mean second moments of the F^{19} absorption line in a single crystal of CaF_2 for three directions of magnetic field in the crystal.

H_0 direction	Experiment	Theory of Van Vleck
100	3.68±0.20 gauss	3.60 gauss
110	2.25±0.20	2.24
111	1.77±0.20	1.53

THE MOMENTS OF THE SHAPE FUNCTION

In the preceding paper, Van Vleck finds expressions for the second and fourth moments of the shape function $g(\nu)$, the $(2n)$th moment being defined as

$$\langle(\Delta\nu)^{2n}\rangle_{Av}=\int_0^\infty g(\nu)(\Delta\nu)^{2n}d\nu. \tag{6}$$

In particular, Van Vleck obtains the second moment in terms of the direction cosines of the magnetic field $\mathbf{H}_0$ with respect to the principal axes of a simple cubic lattice, and he calculates the fourth moment for $\mathbf{H}_0$ along the 100 axis.

The simple cubic lattice of F^{19} nuclei in crystalline CaF_2 offers opportunity for an experimental check of these calculations. The dependence of peak signal strength on magnetic field direction in this crystal has been examined by Purcell, Bloembergen, and Pound.[6] In the present experiments, a cylindrical specimen about 1 cm in diameter and 2.5 cm long was cut from a single crystal of fluorite, the cylindrical axis lying along the 110 crystal direction. The crystal was inserted into the r-f coil of the permanent magnet apparatus described elsewhere,[7] and the derivative of the F^{19} absorption line was plotted for several directions of $\mathbf{H}_0$ in the crystal. One of these experimental curves is reproduced in Fig. 1, the magnetic field being along 100. The second moment may be found directly from this curve by performing a partial integration on the right member of Eq. (6) and recalling that $g(\nu)$ vanishes except in a small frequency interval about ν_0:

$$\langle(\Delta\nu)^{2n}\rangle_{Av}=-\frac{1}{2n+1}\int_0^\infty(\Delta\nu)^{2n+1}\frac{dg(\nu)}{d\nu}d\nu. \tag{7}$$

[6] E. M. Purcell, N. Bloembergen, and R. V. Pound, Phys. Rev. **70**, 988 (1946).
[7] G. E. Pake, J. Chem. Phys. **16**, 327 (1948).

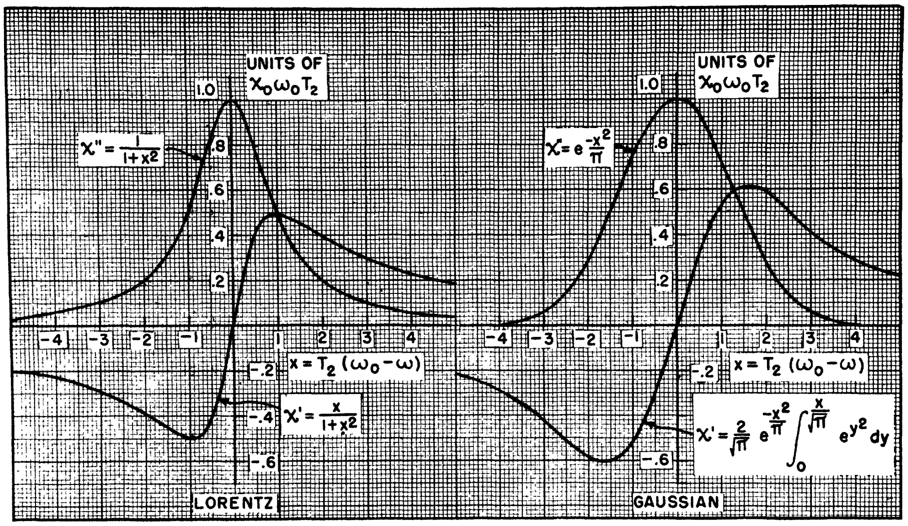

FIG. 2. Nuclear susceptibilities, $\chi = \chi' - i\chi''$.

Root mean square line widths (measured in units of magnetic field rather than frequency) were evaluated numerically using Eq. (7) and curves such as that of Fig. 1 for three directions of $\mathbf{H}_0$ in the CaF_2 crystal. The experimental results are listed in Table I, along with the corresponding values calculated by Van Vleck. The failure of the theoretical width for 111 to fall within the limits of error should not cause undue concern, inasmuch as the relatively large power of $\Delta\nu$ in the integrand of Eq. (7) accentuates the effect on a narrow line of spurious broadening introduced by crystal imperfections or by small errors in crystal orientation.

Figure 1 can be used in a similar way to evaluate the fourth moment, with the result $\langle(\Delta H)^4\rangle_{\text{Av}}^{\frac{1}{4}} = 4.56 \pm 0.20$ gauss. Inasmuch as a considerable part of the error quoted arises from magnetic field calibration, it is perhaps more instructive to consider the ratio $\langle(\Delta H)^4\rangle_{\text{Av}}^{\frac{1}{4}}/\langle(\Delta H)^2\rangle_{\text{Av}}^{\frac{1}{2}}$; the experimental value is 1.24 ± 0.02, compared with 1.25 given by theory.

COMPARISON OF LORENTZ AND GAUSSIAN LINE SHAPES

Bloch[8] has obtained a system of differential equations satisfied by the expectation value of the nuclear magnetization which lead to the Lorentz shape function traditional in the theory of radiation- and collision-broadened spectral lines. For r-f magnetic fields sufficiently weak to preclude saturation, the Bloch susceptibilities are

$$\left.\begin{aligned} \chi''(\omega) &= \chi_0\omega_0 T_2 \frac{1}{1+T_2^2(\omega_0-\omega)^2}, \\ \chi'(\omega) &= \chi_0\omega_0 T_2 \frac{T_2(\omega_0-\omega)}{1+T_2^2(\omega_0-\omega)^2}, \end{aligned}\right\} \tag{8}$$

where $\omega = 2\pi\nu$ is the angular frequency. These susceptibilities are consistent with the Kronig-Kramers relations and with the definitions of Eq. (1).

In attempting to determine line shape by the diagonal sum method, Broer[9] finds a general expression for the $(2n)$th moment:

$$\langle(\Delta\nu)^{2n}\rangle_{\text{Av}} = \frac{\mathrm{Tr}\left[\frac{d^n}{dt^n}S_x\right]^2}{(2\pi)^{2n}\,\mathrm{Tr}[S_x]^2}. \tag{9}$$

Although the shape function would, in principle, be determined by its moments, the highest thus far calculated is the fourth, which Van Vleck obtains in the preceding paper. The practical difficulties in evaluating the higher moments force Broer to follow Heisenberg's theory of ferromagnetism by assuming that $g(\nu)$ is proportional to a Gauss function, $\exp[-\alpha(\Delta\nu)^2]$. Equation (1) requires such an absorption curve to have the form

$$\chi''(\omega) = \chi_0\omega_0 T_2 \exp[-T_2^2(\omega_0-\omega)^2/\pi]. \tag{10}$$

[8] F. Bloch, Phys. Rev. **70**, 460 (1946).

[9] L. J. F. Broer, Physica **10**, 801 (1943).

From Eq. (10) and the first of Eqs. (4) one finds after considerable manipulation that

$$\chi'(\omega)=\chi_0\omega_0T_2\cdot 2\pi^{-\frac{1}{2}}F(\pi^{-\frac{1}{2}}T_2(\omega_0-\omega)), \quad (11)$$

where

$$F(x)=e^{-x^2}\int_0^x e^{y^2}dy. \quad (12)$$

Both Lorentz and Gaussian formulae for $\chi'(\omega)$ should and do reduce to χ_0 at $\omega=0$. To verify this for Eq. (11), one may use $dF/dx=1-2xF$ and the fact that dF/dx is vanishingly small at great distances in frequency from ω_0, in particular, at $\omega=0$.

Both Lorentz and Gaussian shape functions may be linked with idealized physical models, the first of which relies solely on the broadening introduced by oscillatory local field components at the Larmor frequency. By this means neighboring nuclei limit the lifetime of a given nuclear spin state by inducing transitions from it, and mathematical analysis closely parallel to that for collision broadening of ordinary spectral lines[10] would lead to the Lorentz shape function. Such a picture, however, ignores local field static components,** which disperse the resonance values of the large constant magnetic field and which provide the broadening mechanism of the second model: The effective static local field at an absorbing nucleus depends upon the positive or negative excess of its near neighbors with spins aligned in the positive $\mathbf{H}_0$ direction. Spins throughout the sample are assumed to be randomly parallel or antiparallel to $\mathbf{H}_0$ (I is taken $\frac{1}{2}$ for simplicity), and, in the limit of large numbers of near neighbors clustered about each absorbing nucleus, this excess number becomes distributed among the absorbing nuclei according to a Gauss function. The effective local field of the model is essentially proportional to this distribution. Although these models evidently represent much-simplified approximations to reality, they identify the two shape functions, Lorentz and Gaussian, with physical pictures which, however incomplete, may prove helpful until the detailed theory is cast into a form more amenable to calculation.

Figure 2 compares, as functions of $x=T_2(\omega_0-\omega)$, the Lorentz curves of Eq. (8) with the Gaussian curves of Eqs. (10) and (11). Values of the function $F(x)$, which arises in heat-flow problems, are taken from a tabulation by Miller and Gordon.[11] The derivatives of these curves are plotted in Fig. 3, corresponding to the quantities measured directly by experiment. From Figs. 2 and 3, one

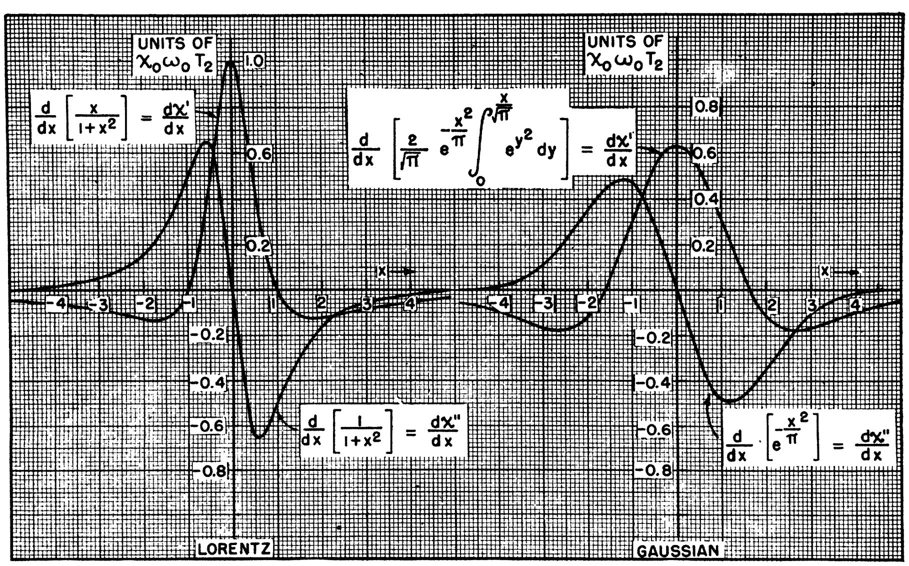

FIG. 3. Derivatives of nuclear susceptibilities, $x=T_2(\omega_0-\omega)$.

[10] J. H. Van Vleck and V. F. Weisskopf, Rev. Mod. Phys. **17**, 227 (1945).
** In Reference 1, pp. 695 and 696, the dipole-dipole Hamiltonian is written in a form which displays terms corresponding to static and Larmor frequency local fields.
[11] W. L. Miller and A. R. Gordon, J. Phys. Chem. **35**, 2875 (1931).

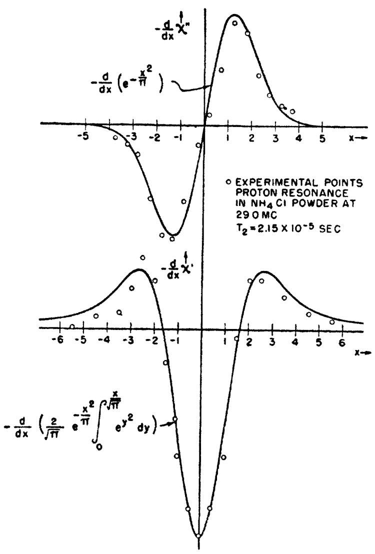

FIG. 4. Negative derivatives of nuclear susceptibilities, $\chi=\chi'-i\chi''$; $x=T_2(\omega_0-\omega)$.

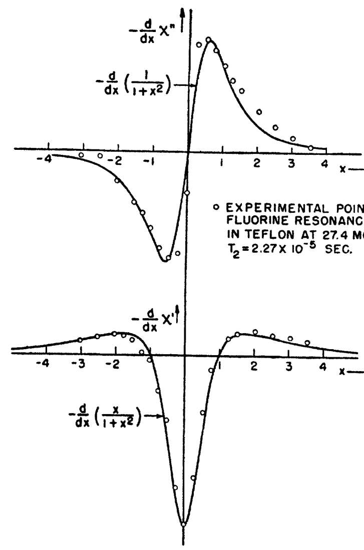

FIG. 5. Negative derivatives of nuclear susceptibilities, $\chi=\chi'-i\chi''$; $x=T_2(\omega_0-\omega)$.

can relate any experimental width measure to $1/T_2$. The Lorentz and Gaussian curves differ most significantly in the ratio R of the large maximum of $d\chi'/dx$ to either small minimum: $R(\text{Lorentz})=8:1$ and $R(\text{Gauss})=3.5:1$. Application of this criterion to an experimental dispersion curve indicates which shape function, if either, seems likely to fit the data.

Figures 4 and 5 show experimental nuclear susceptibilities, measured with the permanent magnet apparatus, which approximate to these two shape functions. The F^{19} resonance in polytetrafluoroethylene (Teflon) at room temperature fits the Bloch curves reasonably well, whereas the proton resonance in NH_4Cl powder at room temperature has $R=3.3$ and more nearly resembles the Gaussian curves. It should be borne in mind that many substances, especially crystals in which "frozen-in" nuclei determine line width and shape, may possess a shape function differing markedly from the two simple ones considered here. Figure 1, for example, does not resemble closely either absorption curve derivative in Fig. 3; the proton dispersion curve for $(NH_4)_2SO_4$ powder has $R=2.5$, and pronounced fine structure has been observed in hydrated crystals.[7]

Facilities for the experimental work here reported, including the large permanent magnet, were provided through a Frederick Gardner Cottrell Special Grant-in-Aid from the Research Corporation.

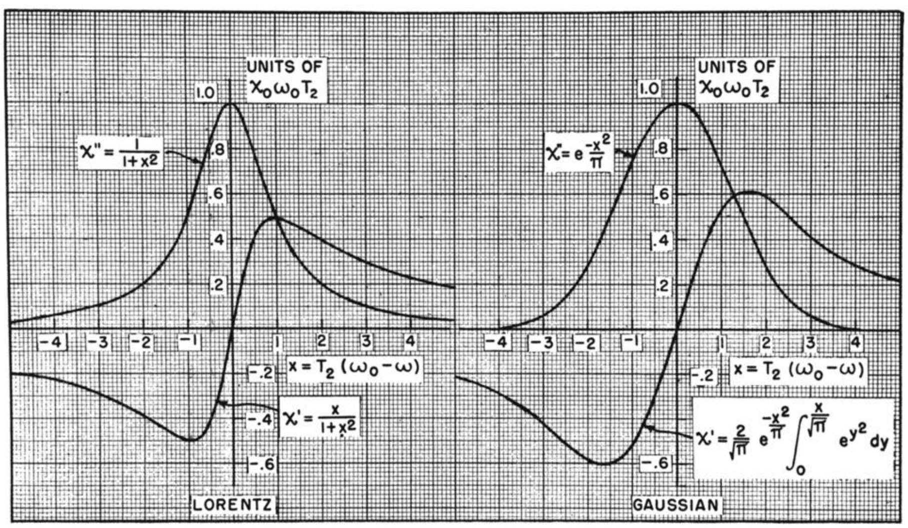

FIG. 2. Nuclear susceptibilities, $\chi = \chi' - i\chi''$.

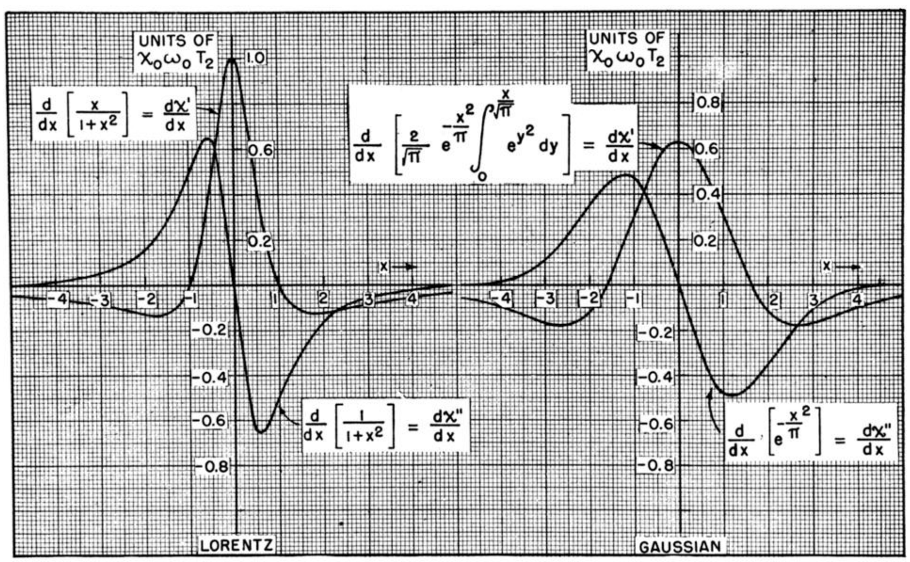

FIG. 3. Derivatives of nuclear susceptibilities, $x = T_2(\omega_0 - \omega)$.